Ambient Backscatter Communication Based Cooperative Relaying for Heterogeneous Cognitive Radio Networks

Muhammed Yusuf ONAY [1,2,3], Ozgur ERTUG [2]

[1] Dept. of EE Engineering, Graduate School of Natural and Applied Sciences, University of Gazi, Maltepe, Ankara, Turkey
[2] Dept. of Electrical and Electronics Engineering, Faculty of Engineering, University of Gazi, Maltepe, Ankara, Turkey
[3] Dept. of Electrical and Electronics Engineering, Faculty of Engineering, University of Hitit, Corum, Turkey

{yusufonay, ertug}@gazi.edu.tr

Abstract. *In this paper, a new network model is proposed to improve the performance of the secondary channel in cognitive radio networks (CRNs) based ambient backscatter communication systems. This model is considered as a cooperative system with multi-secondary transmitter (ST) and multi-relay. The ST backscatters data to both the secondary receiver (SR) and relay. Also it harvests energy from the signal emitted by the primary transmitter (PT) during the busy period. The relay activated by the ST user forwards the information from ST to SR. During the idle period, the PT broadcast is interrupted and ST also performs active data transmission using the energy it has harvested. We aim to maximize the number of data transmitted to the SR. Therefore, how long the ST will perform backscattering, energy harvesting and active data transmission is a problem to be solved. In such cooperative systems with multiple users, the solution of the problem becomes more complex. Therefore, the system model has been mathematically modeled and transformed into an optimization problem, considering that users are transmitting data using time division multiple access (TDMA) and non-orthogonal multiple access (NOMA) techniques. Numerical results showed that higher data rates were achieved in NOMA. Additionally, It has been seen that the proposed model performs better when compared to the existing approaches in the literature, where the ST can only harvest energy and transmit data actively or only transmit data with ambient backscatter communication.*

Keywords

Ambient backscatter communication, cognitive radio networks, cooperative system, relay, energy harvesting, convex optimization

1. Introduction

With the increasing energy demand, wirelessly powered communication systems are getting more and more attention [1], [2]. The user in this communication system can harvest energy using the radio frequency signal in the environment such as TV tower, FM tower, WiFi access, or dedicated signal source (DSS). In the network model, the user located at a certain place spends the time allocated for harvesting in the time block. The number of data that users in the network model send to the receiver in the time allocated to them varies according to the amount of harvested energy from the radio frequency signal. Therefore, the longer the user harvests, the higher the data rate is achieved [3]. Since users will not be able to transmit data to the receiver during the harvesting period, this situation seriously reduces the system performance in terms of transmitted number of data. To overcome this problem, ambient backscatter communication systems, which is a passive communication type in which the user modulates the signal coming from the emitter and scatters it to the receiver, have been proposed and integrated into existing wirelessly powered communication systems [2,4–6].

Ambient backscatter communication can be used especially in low power communication systems such as sensor network and Internet of Things (IoT) [7], [8]. In ambient backscatter communication systems, since the transmitter in the network uses the existing signal in the environment, it does not need a radio frequency signal generator that consumes a significant amount of power, and it does not need a special frequency band because it uses the frequency of the signals in the environment. Backscatter user can work without battery. However, in order to active data transmission to be carried out, a battery must be present in the user's internal structure and this battery must be filled by harvesting energy [9]. Such user is known as hybrid user. Finding out how long the user will do backscatter, active data transmission and harvest in the time block emerges as a problem in wirelessly powered backscatter communication systems. If the system is a multi user model, the problem to find the specified times becomes more complex [10].

There are four main problems in the backscatter communication. Firstly, the data rate of the user is low. Secondly, the energy harvested is small amount when the user is located far from the radio frequency source. Thirdly, If no usable signal is found in the environment, backscattering cannot be

performed. Finally, the dynamic structure of the existing signals in the environment and their variability over time [2]. To overcome these problems, ambient backscatter communication systems are considered together with cognitive radio networks [11–13].

Cognitive radio networks (CRNs) are communication protocol in which the user transmits data using the frequency bands of the signals available in the environment. It basically consists of two parts, the primary channel and the secondary channel. While the transmitter on the primary channel transmits data to its own receiver, the secondary channel completely uses the communication infrastructure of the primary channel [11]. The use of overlay channels, one of the cognitive radio communication techniques, has been examined in this article. In overlay cognitive radio networks, the transmitter in the primary channel cuts off the signal it emits for a certain period of time. This idle period is an opportunity for the user on the secondary channel to actively transmit data. Thus, the user does not create any interference to the receiver on the primary channel. Since the performance of the secondary channel in CRNs systems is directly related to the busy time of the transmitter in the primary channel, system variables in the overlay model should be evaluated by considering parameters such as the transmit power of the PT and the idle period. When the broadcast time of the PT is long, the time during which the user can active data transmit becomes very short and the number of data transmitted to the receiver of the secondary channel drops severely. However, when the overlay CRNs system is considered in the system model with ambient backscatter communication, user can both harvest energy and transmit their data to the secondary receiver by backscattering during the broadcast period of the PT. This improves the performance of the secondary channel [14], [15].

In most of the approaches on cognitive radio network based backscatter communication systems in the literature, the model is considered as a single user, and information is directly backscattered to the receiver. However, in recent studies, cooperative communication techniques have been considered and used extensively to increase the capacity of the system [16–19]. In cooperative systems, relay users are generally used to forward the incoming data to the receiver [20]. It has been shown in many studies in the literature that the use of relay improves system performance [21–25].

In this paper, we aim to improve system performance by using node and relay in CRNs based backscatter communication systems. Through the comparative assesment of the approaches in the literature, the proposed model in this paper is the first approach in which comparative performance analysis of a multi-ST and multi-relay CRNs based ambient backscatter communication system is performed using time division multiple access (TDMA) and non-orthogonal multiple access (NOMA) techniques. First, the proposed system model was formulated, then transformed into an optimization problem. By finding the most suitable backscatter time, harvesting time, active data transmission time, the number

of data reaching the receiver was maximized. The performance of the secondary channel was evaluated according to the change in the idle period, backscatter rate and node / relay number. As a result, the proposed system model significantly increased the system performance of the secondary channel.

The remaining parts of this article are designed as follows: In Sec. 2, basic information about ambient backscatter communication techniques is given and the proposed system model is examined using both TDMA and NOMA techniques. In Sec. 3, the considered system model is mathematically modeled and transformed into an optimization problem. The simulation results obtained according to the optimization problem corresponding to the system model are given in Sec. 4 comparatively. Finally, conclusions and future work are presented in Sec. 5.

2. System Model

Ambient backscatter communication is based on the technique of modulating the incoming signal and sending it to the receiver using antenna impedance mismatch. The antenna reflection coefficient, which determines what kind of modulation will be applied to the signal, is given as follows [5], [26].

$$\Gamma = \frac{X_{\mathrm{L}} - X_{\mathrm{A}}^*}{X_{\mathrm{L}} + X_{\mathrm{A}}^*} = |\Gamma|\, e^{j\theta} \tag{1}$$

where X_{A}, X_{L}, $*$ denote antenna impedance, load impedance, complex conjugate operator, respectively. The signal backscattered from the antenna, with the incoming signal being $S_{\mathrm{c}}(t)$, can be found by the equation $S_{\mathrm{b}}(t) = \Gamma S_{\mathrm{c}}(t)$. Since the reflection coefficient has both amplitude and phase, data can be transmitted on the backscattered signal by both amplitude and phase modulation techniques. Bistate modulation, which is a frequently used and basic modulation, has been used in many studies in the literature to examine the performance analysis of ambient backscatter communication systems.
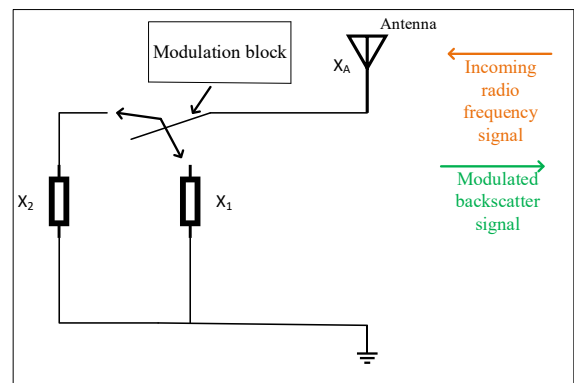
Fig. 1. Bistate modulation for backscatter users in the ambient backscatter communication system.

Notation and Abbreviations	Meaning
DSS	Dedicated signal source (WiFi access point)
PT / PR / PC	Primary transmitter / Primary receiver / Primary channel
SR / SC	Secondary receiver (Gateway) / Secondary channel
ST_i	Secondary transmitter ($i = 1, 2, \ldots, N$)
P^T / P_{DSS}^T	The transmit power of the PT / The transmit power of the DSS
ϵ / η	User energy harvesting efficiency / Relay energy harvesting efficiency
$\lambda / c / f / W$	Signal wavelength / Speed of light / Signal frequency / Primary channel bandwidth
K_i / ψ	Active data transmission efficiency of ST_i / Active data transmission efficiency of Relay
γ_i	Backscatter efficiency of ST_i
B_i^b	Backscatter rate of ST_i
$h_{n,i}, h_{r,j}$	The channel gains between the PT and the ST_i, between the PT and the Relay$_j$, respectively
h_i^{DSS}	The channel gains between the ST_i and the DSS
$g_{ij}, g_{i,SR}$	The channel gains between the Relay$_j$ and the ST_i, between the SR and the ST_i, respectively
$g_{r_j,SR}$	The channel gains between the the Relay$_j$ and the SR
$d_{r,j}, d_{n,i}, d_i^{DSS}$	The distances between the PT and the Relay$_j$, between the ST_i and the PT, between the DSS and the ST_i, respectively
$G_T / G_i^R / G_{DSS,T}$	Antenna gain of PT / Antenna gain of ST_i / Antenna gain of DSS

Tab. 1. Summary of notation and abbreviations.

Bistate modulation is shown in Fig. 1. In impedance matching, the radio frequency signal is absorbed and the signal is not backscattered. This state is represented by bit 0. In impedance mismatch, the signal is backscattered and represented by bit 1. Different modulation techniques have been studied in the literature [5].

In proposed system model, TDMA and NOMA techniques are used and the time block is shown in Fig. 2. The system model is shown in Fig. 3. There are N nodes and M relays in the system model and $N \geq M$ is accepted. Each node (indoor cell [27]) has one the ST user and the DSS. There are two different modes in the time block for both TDMA scenario and NOMA scenario. Backscatter and relay active mode (BRM) is the phase in which active relays are selected in the system model, the ST_i ($i = 1, 2, \ldots, N$) backscatters its data to both the SR and the Relay$_j$ ($j = 1, 2, \ldots, M$), and the Relay$_j$ performs the information forward to the SR. In active data tranmission mode (harvest-then transmit, HTT), the PT broadcast is interrupted. The Relay$_j$ is inactive and the ST_i uses the energy harvested in BRM mode for active data transmission. The time block duration T = 1 s is assumed. HTT and BRM time are shown as α and $1 - \alpha$, respectively. While the ST_i backscatters data during ϕ_i, it transmits actively data for τ_i. Relay selection time is represented by β. The notation and abbreviations are summarized in Tab. 1.

The ST_i can harvest energy from both the signal transmitted from the PT and the signal emitted from the DSS. However, in active data transmission mode, the ST_i uses the DSS to harvest energy, as the PT cuts off signal broadcast in idle period. The DSS in the secondary channel can be considered as WiFi access point. Therefore, since the frequency of the signal emitted by the DSS is high, the power harvested by the ST_i will be low. Each ST_i user harvests energy from the signal transmitted by the DSS, which is in its own cell. The energy stored during the idle period is used for energy consumption in the circuit internal structures in

active data transmission. Therefore, the energy consumed by the ST_i users in the internal circuit structure in active data transmission is neglected. The number of the ST_i in the system model is equal to the number of nodes. The system model in Fig. 3 will be analyzed over the subsystem with one user and one relay and generalized for the whole system. In case of multiple users, the new node and relay user to be included in the system are added to the circle with reference from Node$_1$ and Relay$_1$. Let's assume that the ST_1 user from Node$_1$ indoor zone makes backscatter in ϕ_1 time and only the Relay$_1$ user is active. In backscatter and relay active mode, the backscattered data from the ST_1 user to the SR is given with $R_1^b = \phi_1 B_1^b a_1$ where $a_1 = \gamma_1 g_{1,SR}$. The backscatter rate (B_i^b) of each ST_i is constant and can be changed by adjusting with the resistor-capacitor (RC) elements in the internal circuit structures of the user at appropriate values. Backscatter efficiency γ_1 value is between 0 and 1. If $\gamma_1 = 1$, it means that the signal coming to the user is completely backscattered towards the receiver, otherwise it is not backscattered towards the receiver. The data backscattered to the SR by ST_i user is given by the formula $R_i^b = \phi_i B_i^b a_i$. We assume that the average power P^T of the signal $x(t)$ emitted by the PT in the primary channel. Thus, the equation $\frac{1}{T} \int_0^T |x(t)|^2 = P^T$ can be written. In busy time, ST_i and Relay$_j$ located far enough from PR are assumed not to interfere with PR while they are backscattering and forwarding data, respectively [2], [11].

Relay harvests energy from the signal emitted by the PT during $1 - \alpha$ and uses this energy to decode the information transmitted from the ST_i and transmit it to the SR. During the idle period, not all users in the network model can harvest energy from the PT. Relay$_j$ has initial energy (E_i) in its battery and this energy is not enough to operate during the idle period when the PT is silent. Since it is aimed to increase the performance of the network by using a cooperative system, it is assumed that there is no extra embedded energy source for the Relay$_j$. Each ST_i backscatter its data to relay
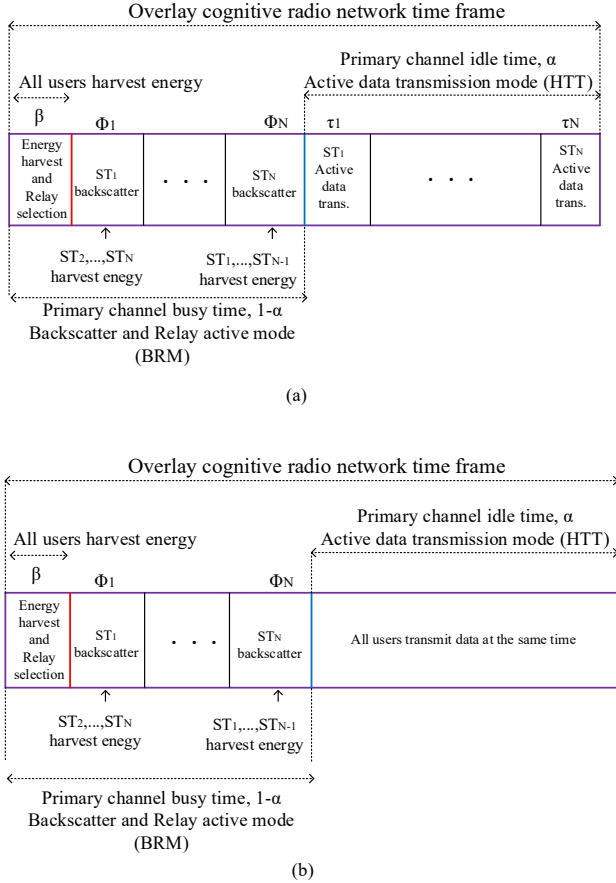
Fig. 2. The system time block. (a) The proposed TDMA scenario; (b) The proposed NOMA scenario.

users close to it. The remote Relay_j user cannot extract the backscattered information because the level of the signal coming to its is low, and it does not waste energy by running itself for the weak signal level and waits to transmit the information of the ST_i located close to it. For this reason, each relay operates according to whether the data received during β is above or below a certain threshold value (R_t). We assumed that SR knows which mode all users are operating, and uses the suitable demodulator circuit for the operating mode of the users to decode the transmitted information. SR also has channel state information (CSI) of both the relay and the ST [15], [28]. In scenarios with simultaneous data transfer in multi-user systems, the receiver can recover the signal transmitted by users using successive interference cancellation (SIC) or joint decoding methods.

In the proposed model, it is assumed that SR and Relay_j use the SIC method [29]. Thus, the interference signal is decoded and removed from the received signal. The channel gains that remain constant throughout the T-second period of the time block but can change in different periods are modeled as quastatic flat-fading. In addition, we assumed that there is a distance-dependent signal attenuation in the system model.

The signal from PT to ST_1 user is given as $\sqrt{h_{n,1}}x$ (noise is neglected here). The backscattered signal $S_1 = \gamma_1 \sqrt{h_{n,1}} x c_1$

is obtained by ST_1. Here c_1 is the user's own signal. In backscatter and relay active mode, The total received signal at the Relay_1 is given as following:

$$y_{r_1} = \gamma_1 \sqrt{h_{n,1}} \sqrt{g_{11}} x c_1 + \sqrt{h_{r,1}} x + n_{r1} +$$
$$\gamma_2 \sqrt{h_{n,2}} \sqrt{g_{21}} x c_2 + \sqrt{h_{r,1}} x + n_{r1} + \ldots$$
$$\gamma_N \sqrt{h_{n,N}} \sqrt{g_{N1}} x c_N + \sqrt{h_{r,1}} x + n_{r1}. \quad (2)$$

The signal received any Relay_j in the system model can be expressed as following:

$$y_{r_j} = \gamma_1 \sqrt{h_{n,1}} \sqrt{g_{1j}} x c_1 + \sqrt{h_{r,j}} x + n_{rj} + \ldots$$
$$\gamma_N \sqrt{h_{n,N}} \sqrt{g_{Nj}} x c_N + \sqrt{h_{r,j}} x + n_{rj} \quad (3)$$

where n_{rj} is a Gaussian noise with zero mean and variance σ^2. The interference signal from PT to Relay_j user is expressed as $\sqrt{h_{r,j}}$.

In TDMA scenario, the ST users do not interference with each other as they perform data transfers in the time allotted to them. As seen in Fig. 2(a), all users harvest energy during β and the relays that will be active are determined. While the ST_i backscatters data to the SR in the duration of ϕ_1, all other users continue to harvest energy. In active data transmission mode, each ST_i user performs active data transmission for τ_i period using the energy they harvest. The ST_i can not backscatter in HTT mode as there is no usable signal in the environment. In BRM mode, ST_i and Relay_j transmit data to SR, while in HTT mode only ST_i transmits data. NOMA, which is highly preferred in 5G and beyond communication systems, allows users to transmit data to the receiver at the same time in networks with multiple transmitters [30], [31]. In addition, users can make efficient use of the frequency spectrum. Due to these advantages, the system model has also considered with the NOMA scenario as shown in Fig. 2(b). In the NOMA scenario, unlike the TDMA scenario, all ST users send their data to the SR at the same time in HTT mode. In this case, ST users interfere with each other. Therefore, this problem is taken into account in the performance analysis.

3. Problem Formulation

The ST_i continues to harvest energy from the PT while backscattering. Although this harvested energy is not sufficient to perform active data transmission, it can be used in necessary circuit operations during backscattering. For this reason, the energy consumed by the user in the internal circuit structure during backscattering is not taken into account in the mathematical equations. Relay users are considered to be active if the number of data received during β period is above a certain threshold value (R_t). Thus, relay users consume the energy they harvest for ST users located close to them. This situation causes the harvested energy to be used more efficiently. Thus, the Quality of Service (QoS) for relay users is guaranteed [32]. Relay_j decodes the backscattered
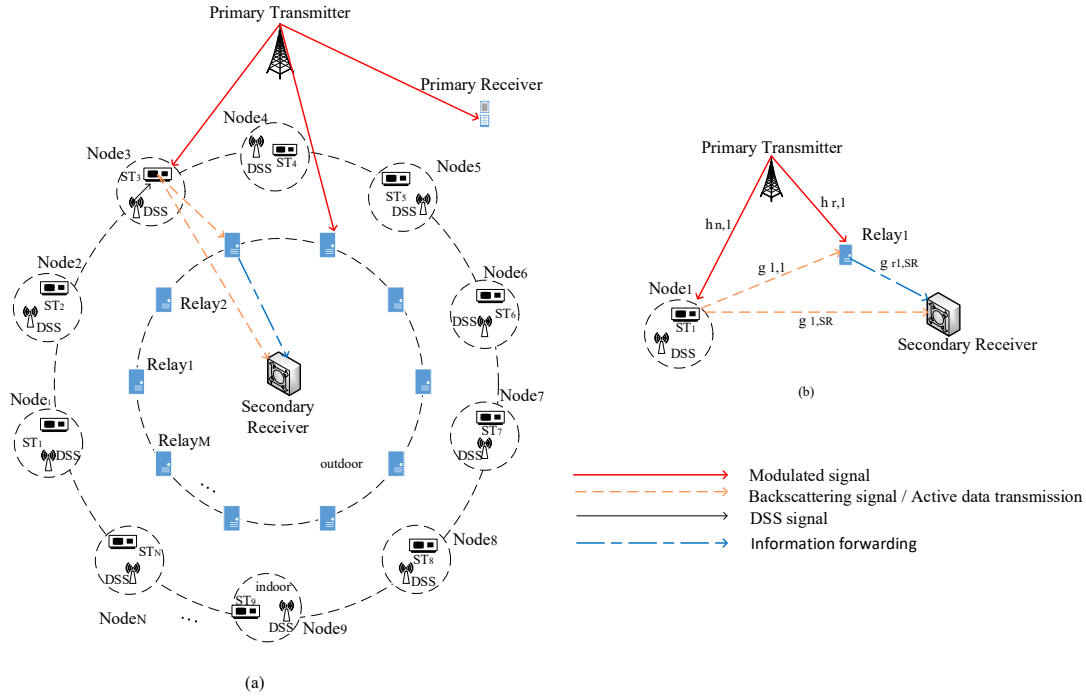
Fig. 3. (a) The proposed system model; (b) The subsystem of the proposed model for $N = 1$, $M = 1$.

signal from the ST_i and information forwards to the SR. In the subsystem given in Fig. 3(b), the number of data reaching the SR when only $Relay_1$ is active is given as following:

$$R_1 = \phi_1 B_1^b a_1 + \phi_1 \psi W \log_2(1 + \gamma_{rl_1}) \tag{4}$$

where γ_{rl_1} is the signal-to-noise ratio (SNR) value for the $Relay_1$ user. In case more than one relay user is active, the number of data reaching SR at time ϕ_1 is expressed as:

$$R_1 = \phi_1 B_1^b a_1 + \sum_{j=1}^{M} \phi_1 \psi W \log_2(1 + \gamma_{rl_j}). \tag{5}$$

The total number of transmitted data to the SR during the busy time in the time block can be expressed by the following formula:

$$R_{sum_1} = \sum_{i=1}^{N} R_i = \sum_{i=1}^{N} \phi_i B_i^b a_i + \sum_{j=1}^{M} \sum_{i=1}^{N} \phi_i \psi W \log_2(1 + \gamma_{rl_j}). \tag{6}$$

The maximum energy harvested by the $Relay_j$ user from the PT is given with $E_j = P^T h_{r,j}(1 - \alpha)\eta$. The average transmit power for the $Relay_j$ can be written as $P_{r_j} = \frac{E_j}{\phi_i}$. Thus, SNR for $Relay_j$ is $\gamma_{rl_j} = \frac{P_{r_j} \, g_{r_j,SR}}{\sigma^2}$, where σ^2 is the noise power at the SR.

The ST_i harvests energy from the radio frequency signal coming to it from the DSS. However, this harvested energy is not sufficient for active data transmission. This low level of stored power is used for backscattering. Therefore, the energy required for the circuit energy consumption in the busy period, which is the backscatter and relay active mode, is not taken into account in the mathematical equations [4].

For the proposed TDMA scenario, the power harvested by each ST_i user from the signal emitted by the PT is given as follows:

$$P_{ST_i}^{PT} = \frac{P^T G_T G_i^R \lambda^2 \epsilon}{(4\pi d_{n,i})^2}. \tag{7}$$

The power harvested by each ST_i user from the signal emitted by the DSS is given as follows:

$$P_{ST_i}^{DSS} = \frac{P_{DSS}^T (G_{DSS,T}) G_i^R \lambda^2 \epsilon}{\left(4\pi d_i^{DSS}\right)^2}. \tag{8}$$

The total harvested power and energy by ST_i from (7) and (8) are obtained as following:

$$\begin{aligned} P_{ST_i} &= P_{ST_i}^{PT} + P_{ST_i}^{DSS}, \\ E_i^h &= \left(P_{ST_i}^{PT} + P_{ST_i}^{DSS}\right)(1 - \alpha - \phi_i - \beta). \end{aligned} \tag{9}$$

The transmit power of the ST_i can be written as $P_i^{tr} = \frac{E_i^h}{\tau_i}$. Thus, during the active data transmission in the idle period, the data rate of the ST_i is given as following:

$$r_i^h = K_i W \log_2\left(1 + \frac{P_i^{tr}}{P_i^0}\right) \tag{10}$$

where $P_i^0 = \frac{N_0}{g_{i,SR}}$, ($N_0$: Noise power). The number of bits transmitted in the idle time by ST_i as following:

$$R_i^h = \tau_i K_i W \log_2\left(1 + \frac{(P_{ST_i}^{PT} + P_{ST_i}^{DSS})(1 - \alpha - \phi_i - \beta)}{\tau_i P_i^0}\right). \tag{11}$$

The total number of bits transmitted in the idle period by all STs as following:

$$R_{\text{sum}_2} = \sum_{i=1}^{N} \tau_i K_i W \log_2 \left(1 + \frac{(P_{\text{ST}_i}^{\text{PT}} + P_{\text{ST}_i}^{\text{DSS}})(1 - \alpha - \phi_i - \beta)}{\tau_i P_i^0} \right). \tag{12}$$

The total number of bits transmitted to the SR in busy and idle time on the secondary channel for TDMA scenario is obtained as follows:

$$R_{\text{sum}} = \sum_{i=1}^{N} \phi_i B_i^b a_i + \sum_{j=1}^{M} \sum_{i=1}^{N} \phi_i \psi W \log_2 (1 + \gamma_{rl_j}) + \\ \sum_{i=1}^{N} \tau_i K_i W \log_2 \left(1 + \frac{(P_{\text{ST}_i}^{\text{PT}} + P_{\text{ST}_i}^{\text{DSS}})(1 - \alpha - \phi_i - \beta) g_{i,\text{SR}}}{\tau_i N_0} \right). \tag{13}$$

We aim to maximize the number of bits transmitted to the SR. Therefore, the following optimization problem can be written:

$$\max_{\phi, \tau} R_{\text{sum}} \rightarrow \text{s.t.} \begin{cases} \sum_{i=1}^{N} \phi_i \leq 1 - \alpha - \beta \\ \phi_i \geq 0 \\ \sum_{i=1}^{N} \tau_i \leq \alpha \\ \tau_i \geq 0 \end{cases} \tag{14}$$

In order to find the solution of the optimization problem given in (14), we will first prove that the R_{sum} function is a concave function.

Lemma 3.1: R_{sum} is the objective function of the (14) problem and the concave function of ϕ and τ. Also, all constraints in (14) are affine. So we can solve the problem with convex optimization techniques.
Proof: Please refer to Appendix A.

For the proposed NOMA scenario, all ST users send their data simultaneously to the SR in the secondary channel during α. The energy harvested by the ST_i is given with $E_i^h = \epsilon \left(P^T (1 - \alpha - \phi_i - \beta) (h_{n,i}) + P_{\text{DSS}}^T (1 - \alpha - \phi_i - \beta) h_i^{\text{DSS}} \right)$. The transmit power of ST_i is $P_i^{\text{tr}} = \frac{E_i^h}{\alpha}$. When the active data transmission in the idle period, the number of bits transmitted by ST_i as following:

$$R_i^h = \alpha K_i W \log_2 \left(1 + \frac{(P_i^{\text{tr}}) g_{i,\text{SR}}}{\left(\sigma^2 + \sum_{j=i+1}^{N} \left(P_j^{\text{tr}} g_{j,\text{SR}} \right) \right)} \right). \tag{15}$$

The total number of bits transmitted to the SR in busy and idle time on the secondary channel for NOMA scenario is obtained as follows:

$$R_{\text{sum}} = \sum_{i=1}^{N} \phi_i B_i^b a_i + \sum_{j=1}^{M} \sum_{i=1}^{N} \phi_i \psi W \log_2 (1 + \gamma_{rl_j}) + \\ \sum_{i=1}^{N} \alpha K_i W \log_2 \left(1 + \frac{(P_i^{\text{tr}}) g_{i,\text{SR}}}{\left(\sigma^2 + \sum_{j=i+1}^{N} \left(P_j^{\text{tr}} g_{j,\text{SR}} \right) \right)} \right). \tag{16}$$

Similarly to the TDMA scenario, the following optimization problem can be written:

$$\max_{\phi, \tau} R_{\text{sum}} \rightarrow \text{s.t.} \begin{cases} \sum_{i=1}^{N} \phi_i \leq 1 - \alpha - \beta \\ \phi_i \geq 0 \\ \alpha \geq 0 \end{cases} \tag{17}$$

The method we used to prove that the objective function in (14) is concave can be applied similarly to (17). Therefore, convex optimization techniques can be used in problem solving. Depending on the formulations given in this section, the algorithm in Appendix B can be used to solve the problems discussed for the proposed TDMA/NOMA scenarios.

4. Simulation Results

The simulation results of the proposed model have compared with the studies [3] and [4] in the literature, when the effect of the variation of the relay number and the idle period time on the total number of bits transmitted was analyzed. In [3], users transmit data only during the idle period (only harvest-then-transmit, HTT), while in [4] users transmit data only by backscatter communication. In addition, energy efficiency (EE), which is used to evaluate the system performance of wireless communication systems and is defined as the ratio of the total number of bits transmitted the receiver during the time frame to the total energy consumed by the system [33–35], has given in the simulation results.

The simulation results have found using the Matlab CVX toolbox. Unless otherwise stated, simulation parameter values are as given in Tab. 2.

The time block duration for both TDMA and NOMA is T = 1. The channel power gain g_{ij} is modelled as $g_{ij} = 10^{-1} \theta d_{ij}^{-\varphi}$, where θ and φ represent channel short-term fading and path-loss exponent, respectively. Since only long-term fading is considered in this study, $\theta = 1$ is accepted. For all other channel gain values, the θ and φ values are the same and the channel gain coefficients have found depending on the distance. Path-loss exponent value is taken as $\varphi = 1$. We set the distance between the ST_i and the Relay$_j$ as $d_{ij} = 3$ m ($i = j$), the distance between the SR and the Relay$_j$ as $d_{\text{r}_j, \text{SR}} = 4$ m, the distance between the ST_i and the SR as $d_{i, \text{SR}} = 5$ m.

B_i^b	300 kbps	α	0.3 s
β	0.1 s	γ_i	0.7
R_t	0.5 kbps	W	6 MHz (TV tower)
f	915 MHz	P^T	17 kW
η	0.8	$\sigma^2 = N_0$	133.59 µW
ϵ	0.7	K_i	0.5
ψ	0.3	$G_T = G_i^R$	6 dBi
P_{DSS}^T	10 dBm	f_{DSS}	2.4 GHz
$d_{n,i} \cong d_{r,j}$	5.16 miles	d_i^{DSS}	0.5 m

Tab. 2. Simulation parameter values.
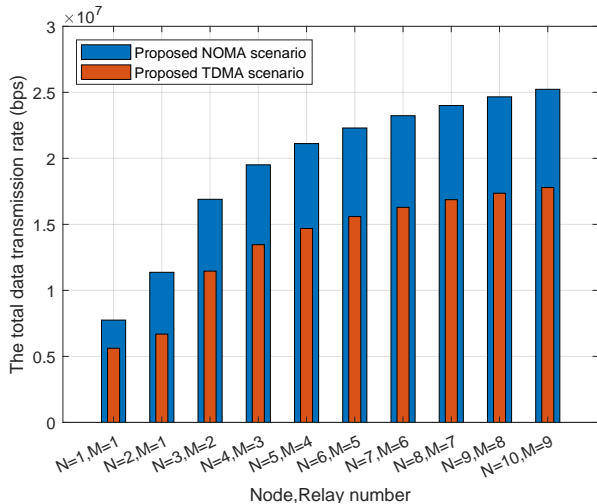
Fig. 4. The total data transmission rate according to the change in the number of node/relay.
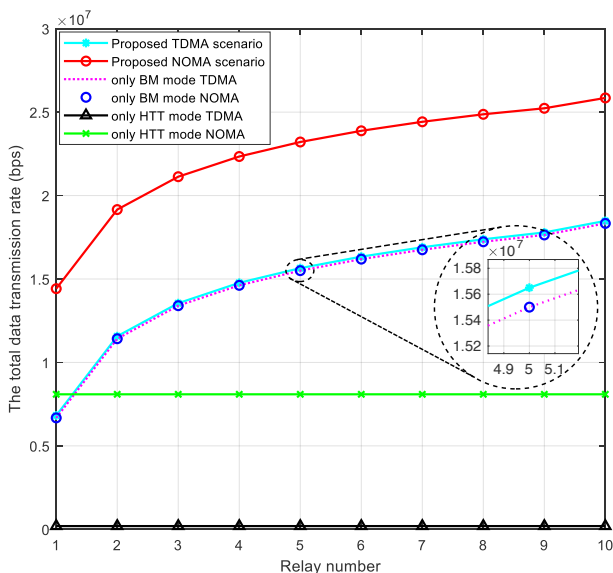
Fig. 5. The total data transmission rate in all scenarios according to the change in the number of relay.

Figure 4 shows that in the case of $N = 1$, $M = 1$, NOMA scenario transmits approximately 1.38 times more data per second than TDMA scenario. This is because in the single-user NOMA scenario, data is transmitted during the active data transmission period ($\alpha = 0.3$) and the $\sum_{j=i+1}^{N} \left(P_j^{\text{tr}} g_{j,\text{SR}} \right)$ term in (16) becomes zero. So there is no interference. The TDMA scenario, on the other hand, prefers only BRM mode to maximize the transmitted data when $N = 1$, $M = 1$. For $N = 2$, $M = 1$, the TDMA scenario uses both BRM and HTT mode. Since there is no interference to the second user in the NOMA scenario, the backscatter time is kept short and the number of data transmitted during active data transmission is increased. Because, if ϕ_2 is short, the second user will harvest more energy, and this energy will be used during α. Backscatter time is allocated to each user according to the number of relays activated by the users. The difference

between NOMA and TDMA in regard to number of data increased to 1.69 times. In the NOMA scenario, not changing the number of relays and adding a user who transmits data actively for the duration α increased the performance difference with the TDMA scenario. From $N = 3$, $M = 2$ to $N = 10$, $M = 9$, the performance difference between the two scenarios decreases and becomes 1.42 for $N = 10$, $M = 9$. As the number of relay increases, the TDMA scenario uses the BRM mode more effectively and a faster increase is observed in the number of data transmitted to the SR per unit time. The reason for the slower increase in the NOMA scenario can be said to be the users' interference with each other. Increasing the number of users and relays has improved performance in terms of the number of data transmitted to the SR. The distance between users and relays gets shorter as the new relay and user are incorporated into the system model. The number of relays activated by ST in BRM mode also increases. However, since the ϕ_i and τ_i times allocated to each user will be shortened in both TDMA and NOMA time blocks, the rate of increase in the total number of data reaching the receiver decreases as seen in Fig. 4.

Figure 5 shows the variation of the total data transmission rate according to the number of relays. In case of $M = 1$, the NOMA scenario provides 2.11 times more data transfer than the TDMA scenario, while this difference decreases to 1.39 when $M = 10$. This result shows that users (ST_i) use relays (Relay_j) more effectively in TDMA scenario. The proposed NOMA scenario shows the best performance for all possible situations. After $M = 2$, we achieved higher data rates in the proposed TDMA scenario compared to only BM and only HTT mode. In only BM mode, Relay_j does not work during HTT mode as it can not harvest for α. ST_i can backscatter during $1 - \alpha$. According to (13) and (16), we see that the performance obtained from only BM mode TDMA and only BM mode NOMA is the same. In only HTT mode, the ST_i does not backscatter and only harvests energy for $1 - \alpha$. In only HTT mode NOMA and only HTT mode TDMA cases, system performance remains constant as it does not depend on the number of relays.

In Fig. 6, the system model is assumed as $N = 5$, $M = 5$ and the variation of the data rate according to the primary channel idle period is analyzed. The proposed NOMA scenario gives the best performance until the idle period of the primary channel is 78.26% of the entire time block. From the critical value of $\alpha = 0.78$ to 0.8, the only HTT NOMA mode gives the best results (at the critical value of $\alpha = 0.78$, the proposed NOMA and the only HTT NOMA have the same data rate). In the proposed TDMA scenario, slightly higher data rate is obtained for each value of the idle period compared to the only BM TDMA/NOMA situation. In the proposed TDMA, the highest data rates are obtained up to the critical point of $\alpha = 0.51$ compared to the other four cases except the proposed NOMA scenario. At the critical point of $\alpha = 0.51$, the same data rate is reached in the case of only HTT NOMA and proposed TDMA scenario. The only HTT NOMA and only BM TDMA/NOMA have the same
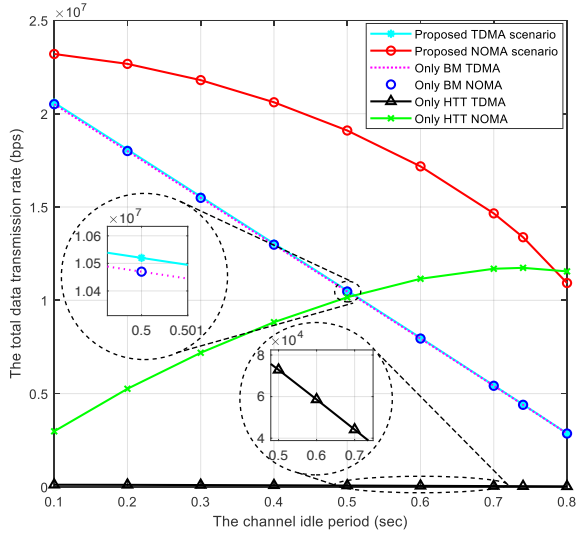
Fig. 6. The total data transmission rate in all scenarios under different values of the channel idle period.
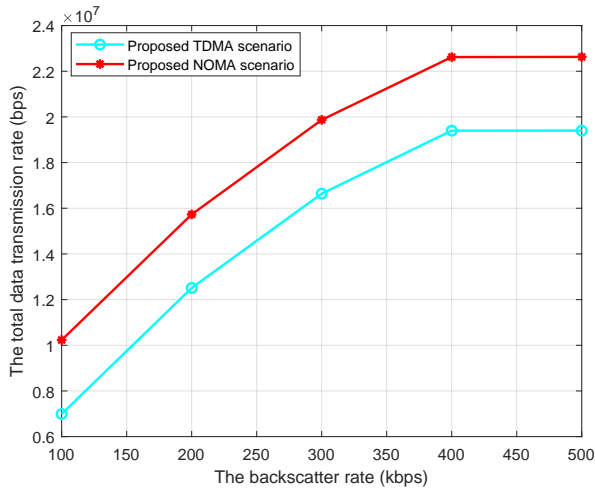
Fig. 7. The total data transmission rate under different values of the backscatter rate.

performance at $\alpha = 0.5$. In case of only HTT NOMA, there is an increase in data rate up to $\alpha = 0.74$. However, after this value, it is seen from Fig. 6 that there is a slight decrease in the number of data transmitted to the receiver per unit time. In the problem of maximizing the number of data transmitted the receiver, we determined that the data transmission rate decreased from 116.29 kbps to 29.52 kbps when the only HTT TDMA scenario was used. Figure 6 shows that the proposed TDMA scenario decreases faster than the proposed NOMA scenario. We have seen that for the proposed TDMA, $R_{\text{sum}} = 20.59$ Mbps at $\alpha = 0.1$, $R_{\text{sum}} = 2.87$ Mbps at $\alpha = 0.8$, for the proposed NOMA, $R_{\text{sum}} = 23.2$ Mbps at $\alpha = 0.1$, $R_{\text{sum}} = 10.92$ Mbps at $\alpha = 0.8$. The reason for this result can be explained as follow: At $\alpha = 0.1$, ST_i and Relay_j use BRM mode effectively because ST_i does not have enough active data transmission time to use the energy harvested. As the value of α increases, the ST_i begins to take advantage of the HTT period effectively. All ST_i users transmit data in NOMA for α time.

That is, the HTT period is more preferred in the proposed NOMA than in the proposed TDMA. Therefore, as α increases, the proposed NOMA decreases more slowly than the proposed TDMA in terms of the total data transmission rate. If the primary channel idle period is increased, the time users can harvest energy in BRM mode is reduced. Although α increases, the number of data transmitted in the HTT period diminish as the harvested energy decreases. Additively, as the duration of the BRM period shortens, serious decreases are observed in the number of data. Since the proposed TDMA uses BRM mode more effectively, the decrease in the number of data is more than the proposed NOMA.

In Fig. 7, the system model is assumed as $N = 8$, $M = 8$. We set the distance between the ST_i and the Relay_j as $d_{ij} = 0.7$ m $(i = j)$, the distance between the SR and the Relay_j as $d_{r_j, \text{SR}} = 1.5$ m, the distance between the ST_i and the SR as $d_{i, \text{SR}} = 2$ m, $R_t = 1$ kbps. Increasing the backscatter rate of the ST_i activates more relays in the system model and improves system performance due to the $\sum_{j=1}^{M} \phi_1 \psi W \log_2(1 + \gamma_{\text{rl}_j})$ term. Since the proposed TDMA scenario spends a significant amount of time using the relay channel, when the backscatter rate is $B_i^{\text{b}} = 100$ kbps and $B_i^{\text{b}} = 500$ kbps, there is 1.46 and 1.16 times difference between the two scenarios, respectively. Since all relays are active for $R_t = 1$ kbps at $N = 8$, $M = 8$, a slight increase in data rate is observed after $B_i^{\text{b}} = 400$ kbps in both cases.

Figure 8 shows the variation of the system energy efficiency according to the number of node/relay. As shown in Fig. 4, the number of data transmitted to the receiver in the proposed NOMA is higher than in the proposed TDMA. For this reason, higher energy efficiency has been achieved in NOMA. In the case of $N = 2$, $M = 1$, the number of data reaching the receiver increased and the highest energy efficiency was obtained in both cases. With the new node and relay added, the total energy consumed by the users in the system increases. The increase in the total data transmission rate transmitted to the receiver slows down. This causes a decrease in energy efficiency. For TDMA, using the relay channel more effectively and increasing the energy consumed by the relays give lower energy efficiency than NOMA.

In Fig. 9, the change of the system energy efficiency according to the channel idle period is given. The system model is assumed as $N = 5$, $M = 5$. As the channel idle time increases, the energy efficiency increases for the proposed NOMA and decreases for the proposed TDMA. As can be seen in Fig. 6, since the active time of the relay users decreases, the number of data obtained for proposed TDMA decreases very quickly compared to proposed NOMA. The absence of a usable radio frequency signal in the environment reduces the total energy harvested by the system, in other words the energy consumed. Since this situation seriously reduces the number of data transmitted to the receiver, the energy efficiency for the proposed TDMA decreases. The total data rate obtained in NOMA decreases slowly. In addition, since NOMA uses the HTT mode effectively, the increase in the idle period causes an increase in energy efficiency.
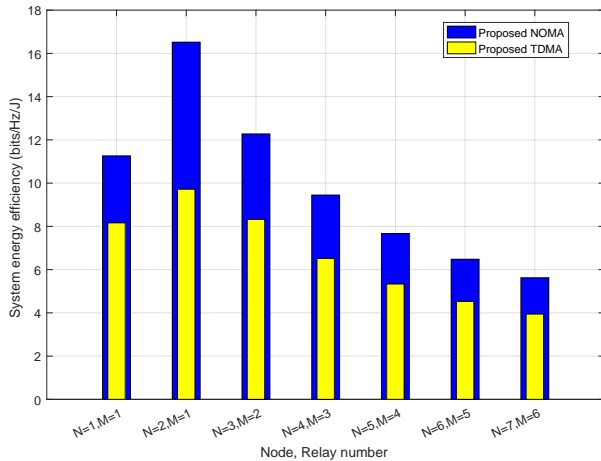
Fig. 8. The variation of the system energy efficiency according to the number of node/relay.
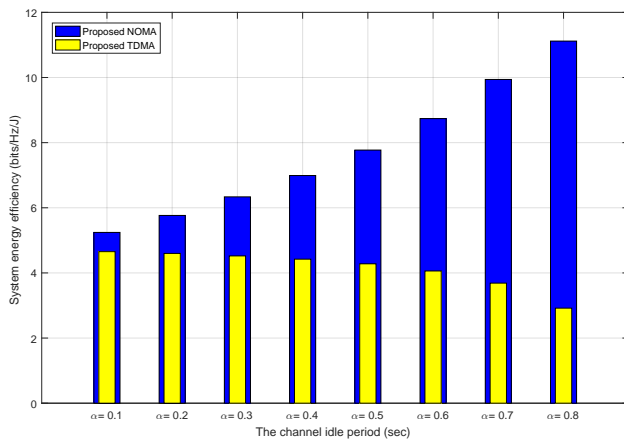
Fig. 9. The change of the system energy efficiency according to the channel idle period.

5. Conclusions and Future Work

In this work, the performance of the secondary channel in terms of data rate in the backscatter system is analyzed. Since PT becomes silent in a certain part of the time block, the system is considered as overlay cognitive networks. The system model with multi-ST and multi-relay has been mathematically modeled and transformed into an optimization problem, considering that users are transmitting data using time division multiple access (TDMA) and non-orthogonal multiple access (NOMA) techniques. Numerical results show that the proposed NOMA scenario is more efficient than the TDMA scenario. When the proposed system is considered in terms of both scenarios, higher data rates have been achieved than similar approaches in the literature which can be used in IoT applications such as smart home/city as wireless sensor networks [2]. For future work, we will consider the system as underlay cognitive radio network and examine performance of the secondary channel.

References

[1] AKYILDIZ, I. F., KAK, A., NIE, S. 6G and Beyond: The future of wireless communications systems. *IEEE Access*, 2020, vol. 8, p. 133995–134030. DOI: 10.1109/ACCESS.2020.3010896

[2] WU, W., WANG, X., HAWBANI, A., et al. A survey on ambient backscatter communications: Principles, systems, applications, and challenges. *Computer Networks*, 2022, vol. 216, p. 1–17. DOI: 10.1016/j.comnet.2022.109235

[3] JU, H., ZHANG, R. Throughput maximization in wireless powered communication networks. *IEEE Transactions on Wireless Communications*, 2014, vol. 13, no. 1, p. 418–428. DOI: 10.1109/TWC.2013.112513.130760

[4] LIU, V., PARKS, A., TALLA, V., et al. Ambient backscatter: Wireless communication out of thin air. *Association for Computing Machinery*, 2013, vol. 43, no. 4, p. 39–50. DOI: 10.1145/2534169.2486015

[5] XU, C., YANG, L., ZHANG, P. Practical backscatter communication systems for battery-free internet of things: A tutorial and survey of recent research. *IEEE Signal Processing Magazine*, 2018, vol. 35, no. 5, p. 16–27. DOI: 10.1109/MSP.2018.2848361

[6] HUYNH, N. V., HOANG, D. T., LU, X., et al. Ambient backscatter communications: A contemporary survey. *IEEE Communications Surveys Tutorials*, 2018, vol. 20, no. 4, p. 2889–2922. DOI: 10.1109/COMST.2018.2841964

[7] LIU, X., GAO, Y., HU, F. Optimal time scheduling scheme for wireless powered ambient backscatter communications in IoT networks. *IEEE Internet of Things Journal*, 2019, vol. 6, no. 2, p. 2264–2272. DOI: 10.1109/JIOT.2018.2889700

[8] MURATKAR, T. S., BHURANE, A., SHARMA, P., et al. Ambient backscatter communication with mobile RF source for IoT-based applications. *AEU - International Journal of Electronics and Communications*, 2021, vol. 141, p. 1–11. DOI: 10.1016/j.aeue.2021.153974

[9] ONAY, M. Y., DULEK, B. Performance analysis of TV, FM and WiFi signals in backscatter communication networks. In *27th Signal Processing and Communications Applications Conference (SIU)*. Sivas (Turkey), 2019, p. 1–4. DOI: 10.1109/SIU.2019.8806350

[10] LYU, B., YANG, Z., GUI, G., et al. Wireless powered communication networks assisted by backscatter communication. *IEEE Access*, 2017, vol. 5, p. 7254–7262. DOI: 10.1109/ACCESS.2017.2677521

[11] HOANG, D. T., NIYATO, D., WANG, P., et al. Ambient backscatter: A new approach to improve network performance for RF-Powered cognitive radio networks. *IEEE Transactions on Communication*, 2017, vol. 65, no. 9, p. 3659–3674. DOI: 10.1109/TCOMM.2017.2710338

[12] KISHORE, R., GURUGOPINATH, S., SOFOTASIOS, P. C., et al. Opportunistic ambient backscatter communication in RF-powered cognitive radio networks. *IEEE Transactions on Cognitive Communications and Networking*, 2019, vol. 5, no. 2, p. 413–426. DOI: 10.1109/TCCN.2019.2907090

[13] LI, Q. Sum-throughput maximization in backscatter communication-based cognitive networks. *Wireless Communications and Mobile Computing*, 2022, vol. 2022, p. 1–11. DOI: 10.1155/2022/7768588

[14] ONAY, M. Y., DURAK, M. H., ERTUG, O. Transmission performance analysis of cognitive radio based backscatter communication systems. In *13th International Conference on Electrical and Electronics Engineering (ELECO)*. Bursa (Turkey), 2021, p. 1–5. DOI: 10.23919/ELECO54474.2021.9677814

[15] HOANG, D. T., NIYATO, D., WANG, P., et al. Optimal time sharing in RF-powered backscatter cognitive radio networks. In *IEEE International Conference on Communications (ICC)*. Paris (France), 2017, p. 1–6. DOI: 10.1109/ICC.2017.7996410

[16] LYU, B. T., YANG, Z., XIE, T., et al. Optimal time allocation in relay assisted backscatter communication systems. In *IEEE 87th Vehicular Technology Conference (VTC Spring)*. Porto (Portugal), 2018, p. 1–5. DOI: 10.1109/VTCSpring.2018.8417655

[17] GAO, X., NIYATO, D., YANG, K., et al. Cooperative scheme for backscatter-aided passive relay communications in wireless-powered D2D networks. *IEEE Internet of Things Journal*, 2022, vol. 9, no. 1, p. 152–164. DOI: 10.1109/JIOT.2021.3096652

[18] WANG, W.-J., XU, K., YAN, Y., et al. Relay selection-based cooperative backscatter transmission with energy harvesting: Throughput maximization. *IEEE Wireless Communications Letters*, 2022, vol. 11, no. 7, p. 1533–1537. DOI: 10.1109/LWC.2022.3179019

[19] ZHENG, C., ZHOU, W., LU, X. Energy efficiency maximization in the wireless-powered backscatter communication networks with DF relaying. *Wireless Communications and Mobile Computing*, 2022, vol. 2022, p. 1–12. DOI: 10.1155/2022/2806423

[20] CHEN, H., LI, Y., REBELATTO, J. L., et al. Harvest-then-cooperate: Wireless-powered cooperative communications. *IEEE Transactions on Signal Processing*, 2015, vol. 63, no. 7, p. 1700–1711. DOI: 10.1109/TSP.2015.2396009

[21] LI, D. Backscatter communication via harvest-then-transmit relaying. *IEEE Transactions on Vehicular Technology*, 2020, vol. 69, p. 6843–6847. DOI: 10.1109/TVT.2020.2991227

[22] SIROJUDDIN, A., NZIMA, V., SINGH, K., et al. Backscatter-aided relaying for next-generation wireless communications with SWIPT. *IEEE Access*, 2021, vol. 9, p. 159093–159104. DOI: 10.1109/ACCESS.2021.3131211

[23] HUSSAIN, Q., SOHAIB, S. Full duplex relaying in non orthogonal multiple access system with advanced successive interference cancellation. *Radioengineering*, 2020, vol. 29, p. 654–663. DOI: 10.13164/re.2020.0654

[24] YUNIDA, Y., MUHARAR, R., AWAY, Y., et al. Efficient relay selection algorithm for non-orthogonal amplify-and-forward cooperative systems over block-fading channels. *Radioengineering*, 2020, vol. 29, p. 386–396. DOI: 10.13164/re.2020.0386

[25] NGUYEN, K.-T., DO, D.-T., VOZNAK, M. An optimal analysis in wireless powered full-duplex relaying network. *Radioengineering*, 2017, vol. 26, p. 369–375. DOI: 10.13164/re.2017.0369

[26] BLETSAS, A., ALEVIZOS, P. N., VOUGIOUKAS, G. The art of signal processing in backscatter radio for μW (or less) internet of things: Intelligent signal processing and backscatter radio enabling batteryless connectivity. *IEEE Signal Processing Magazine*, 2018, vol. 35, no. 5, p. 28–40. DOI: 10.1109/MSP.2018.2837678

[27] KIM, S. H., KIM, D. I. Hybrid backscatter communication for wireless-powered heterogeneous networks. *IEEE Transactions on Wireless Communications*, 2017, vol. 16, no. 10, p. 6557–6570. DOI: 10.1109/TWC.2017.2725829

[28] SUN, J., ZHANG, S., CHI, K. Optimal time allocation for throughput maximization in backscatter assisted wireless powered communication networks. *IET Communications*, 2021, vol. 15, no. 12, p. 1620–1631. DOI: 10.1049/cmu2.12175

[29] DIAMANTOULAKIS, P. D., PAPPI, K. N., DING, Z., et al. Wireless-powered communications with non-orthogonal multiple access. *IEEE Transactions on Wireless Communication*, 2016, vol. 15, no. 12, p. 8422–8436. DOI: 10.1109/TWC.2016.2614937

[30] YANG, G., XU, X., LIANG, Y.-C. Resource allocation in NOMA-enhanced backscatter communication networks for wireless powered IoT. *IEEE Wireless Communications Letters*, 2020, vol. 9, no. 1, p. 117–120. DOI: 10.1109/LWC.2019.2944369

[31] LYU, B. T., YANG, Z., GUI, G., et al. Optimal time allocation in backscatter assisted wireless powered communication networks. *Sensors*, 2017, vol. 17, no. 6, p. 1–11. DOI: 10.3390/s17061258

[32] LU, X., NIYATO, D., JIANG, H., et al. Ambient backscatter assisted wireless powered communications. *IEEE Wireless Communications*, 2018, vol. 25, no. 2, p. 170–177. DOI: 10.1109/MWC.2017.1600398

[33] COSTA, M., EPHREMIDES, A. Energy efficiency versus performance in cognitive wireless networks. *IEEE Journal on Selected Areas in Communications*, 2016, vol. 34, no. 5, p. 1336–1347. DOI: 10.1109/JSAC.2016.2520219

[34] MILI, M. R., MUSAVIAN, L., HAMDI, K. A., et al. How to increase energy efficiency in cognitive radio networks. *IEEE Transactions on Communications*, 2016, vol. 64, no. 5, p. 1829–1843. DOI: 10.1109/TCOMM.2016.2535371

[35] HU, H., ZHANG, H., LIANG, Y.-C. On the spectrum- and energy-efficiency tradeoff in cognitive radio networks. *IEEE Transactions on Communications*, 2016, vol. 64, no. 2, p. 490–501. DOI: 10.1109/TCOMM.2015.2505281

About the Authors . . .

Muhammed Yusuf ONAY was born in Batman, Turkey in 1992. He received his M.Sc. from Hacettepe University in 2019. His research interests include ambient backscatter communication, cognitive radio networks, wireless communication, signal processing. He is currently a Ph.D. student in Electrical and Electronics Engineering Dept. at Gazi University, Ankara, Turkey, where he is working as a Research Assistant since 2019.

Ozgur ERTUG was born in Ankara, Turkey in 1975. He received his M.Sc. from Rice University in 1999 and Ph.D. from Middle East Technical University in 2005. He is currently working as an Associate Professor in Electrical and Electronics Engineering Dept. of Gazi University. His main research interests lie in algorithm and architecture design as well as theoretical and simulation-based performance analysis of software-defined telecommunication and defense systems.

Appendix A: The Proof of Lemma 3.1

Before we begin to prove that Equation (14) is concave, let's define the following statements:

$$y_1 = B_i^{\mathrm{b}} a_1, \ y_2 = \psi W, \ y_3 = K_i W,$$

$$y_4 = \frac{P_{\mathrm{ST}_i} g_{i,\mathrm{SR}}}{N_0}, \ y_5 = 1 - \alpha - \beta, \tag{A1}$$

$$z_j = \frac{E_j g_{\mathrm{r}_j,\mathrm{SR}}}{\sigma^2}, \ (z_1 = z_2 = \cdots = z_M = z)$$

where the numbers $y_1, y_2, y_3, y_4, y_5, z$ are non-negative numbers. Let's define the variables of the optimization problem as $\mathbf{x} = [x_1, \ldots, x_N, x_{N+1}, \ldots, x_{N+N}]^{\mathrm{T}} = [\phi_1, \ldots, \phi_N, \tau_1, \ldots, \tau_N]^{\mathrm{T}}$. The objective function to prove that it is concave over $\mathbf{x}$ is as follows:

$$R_{\mathrm{sum}}(\mathbf{x}) = \sum_{i=1}^{N} y_1 x_i + \sum_{j=1}^{M} \sum_{i=1}^{N} y_2 x_i \log_2\left(1 + \frac{z}{x_i}\right) +$$

$$\sum_{i=1}^{N} y_3 x_{N+i} \log_2\left(1 + \frac{(y_5 - x_i) y_4}{x_{N+i}}\right). \tag{A2}$$

The gradient vector of the $R_{\mathrm{sum}}(\mathbf{x})$ function is as follows:

$$\nabla R_{\mathrm{sum}}(\mathbf{x}) = \left[\frac{\partial R_{\mathrm{sum}}}{\partial x_1}, \ldots, \frac{\partial R_{\mathrm{sum}}}{\partial x_N}, \frac{\partial R_{\mathrm{sum}}}{\partial x_{N+1}}, \ldots, \frac{\partial R_{\mathrm{sum}}}{\partial x_{N+N}}\right]. \tag{A3}$$

For backscatter and relay active mode times:

$$\frac{\partial R_{\mathrm{sum}}}{\partial x_1} = y_1 + \left(\frac{y_3 x_{N+1}}{\ln 2}\left(\frac{-y_4}{x_{N+1} + (y_5 - x_1) y_4}\right)\right) +$$

$$M\left\{y_2 \log_2\left(1 + \frac{z}{x_1}\right) + y_2 x_1 \log_2 e\left(\frac{-z}{x_1(x_1 + z)}\right)\right\}.$$

$$\frac{\partial R_{\mathrm{sum}}}{\partial x_N} = y_1 + \left(\frac{y_3 x_{N+N}}{\ln 2}\left(\frac{-y_4}{x_{N+N} + (y_5 - x_N) y_4}\right)\right) +$$

$$M\left\{y_2 \log_2\left(1 + \frac{z}{x_N}\right) + y_2 x_N \log_2 e\left(\frac{-z}{x_N(x_N + z)}\right)\right\}. \tag{A4}$$

For active data tranmissions times:

$$\frac{\partial R_{\mathrm{sum}}}{\partial x_{N+1}} = \frac{y_3}{\ln 2}\left(\frac{-(y_5 - x_1) y_4}{(x_{N+1}) + (y_5 - x_1) y_4}\right) +$$

$$y_3 \log_2\left(1 + \frac{(y_5 - x_1) y_4}{x_{N+1}}\right).$$

$$\frac{\partial R_{\mathrm{sum}}}{\partial x_{N+N}} = \frac{y_3}{\ln 2}\left(\frac{-(y_5 - x_N) y_4}{(x_{N+N}) + (y_5 - x_N) y_4}\right) +$$

$$y_3 \log_2\left(1 + \frac{(y_5 - x_N) y_4}{x_{N+N}}\right). \tag{A5}$$

The Hessian matrix of the objective function R_{sum} is as follows:

$$\mathbf{H} = \begin{bmatrix} \frac{\partial^2 R}{\partial^2 x_1} & \cdots & \frac{\partial^2 R}{\partial x_1 \partial x_N} & \cdots & \frac{\partial^2 R}{\partial x_1 \partial x_{N+N}} \\ \vdots & \ddots & \vdots & \ddots & \vdots \\ \frac{\partial^2 R}{\partial x_1 \partial x_N} & \cdots & \frac{\partial^2 R}{\partial^2 x_N} & \cdots & \frac{\partial^2 R}{\partial x_N \partial x_{N+N}} \\ \vdots & \ddots & \vdots & \ddots & \vdots \\ \frac{\partial^2 R}{\partial x_{N+N} \partial x_1} & \cdots & \frac{\partial^2 R}{\partial x_{N+N} \partial x_N} & \cdots & \frac{\partial^2 R}{\partial^2 x_{N+N}} \end{bmatrix}_{2N \times 2N} \tag{A6}$$

The Hessian matrix is a symmetric matrix and it is sufficient to find the following expressions.

$$\frac{\partial^2 R}{\partial^2 x_1} = M\left\{\frac{-2y_2 z}{(\ln 2) x_1 (x_1 + z)} + \frac{y_2 x_1 z}{\ln 2}\left(\frac{2x_1 + z}{(x_1^2 + x_1 z)^2}\right)\right\} +$$

$$\frac{-y_3 y_4^2 (x_{N+1})}{\ln 2 \left(x_{N+1} + (y_5 - x_1) y_4\right)^2}.$$

$$\frac{\partial^2 R}{\partial^2 x_N} = M\left\{\frac{-2y_2 z}{(\ln 2) x_N (x_N + z)} + \frac{y_2 x_N z}{\ln 2}\left(\frac{2x_N + z}{(x_N^2 + x_N z)^2}\right)\right\} +$$

$$\frac{-y_3 y_4^2 (x_{N+N})}{\ln 2 \left(x_{N+N} + (y_5 - x_N) y_4\right)^2}.$$

$$\frac{\partial^2 R}{\partial^2 x_{N+1}} = \frac{-y_3 (y_5 - x_1) y_4}{\ln 2 \left(x_{N+1}\right)\left(x_{N+1} + (y_5 - x_1) y_4\right)} +$$

$$\frac{y_3 (y_5 - x_1) y_4}{\ln 2 \left(x_{N+1} + (y_5 - x_1) y_4\right)^2}.$$

$$\frac{\partial^2 R}{\partial^2 x_{N+N}} = \frac{-y_3 (y_5 - x_N) y_4}{\ln 2 \left(x_{N+N}\right)\left(x_{N+N} + (y_5 - x_N) y_4\right)} +$$

$$\frac{y_3 (y_5 - x_N) y_4}{\ln 2 \left(x_{N+N} + (y_5 - x_N) y_4\right)^2}.$$

$$\frac{\partial^2 R}{\partial x_1 \partial x_{N+1}} = \frac{\partial^2 R}{\partial x_{N+1} \partial x_1} = \frac{-y_4^2 y_3}{\ln 2}\left(\frac{y_5 - x_1}{(x_{N+1} + (y_5 - x_1) y_4)^2}\right).$$

$$\frac{\partial^2 R}{\partial x_N \partial x_{N+N}} = \frac{\partial^2 R}{\partial x_{N+N} \partial x_N}$$

$$= \frac{-y_4^2 y_3}{\ln 2}\left(\frac{y_5 - x_N}{(x_{N+N} + (y_5 - x_N) y_4)^2}\right). \tag{A7}$$

Then, given an random real vector $\mathbf{v} = [v_1, \ldots, v_N, v_{N+1}, \ldots, v_{N+N}]^{\mathrm{T}}$ we have $\mathbf{v}^{\mathrm{T}} \mathbf{H} \mathbf{v} =$

$$= \left(\frac{v_1^2 \partial^2 R}{\partial^2 x_1} + \frac{(v_1)(v_{N+1}) \partial^2 R}{\partial x_{N+1} \partial x_1}\right) + \cdots$$

$$\left(\frac{v_N^2 \partial^2 R}{\partial^2 x_N} + \frac{(v_N)(v_{N+N}) \partial^2 R}{\partial x_{N+N} \partial x_N}\right) +$$

$$\left(\frac{v_{N+1}^2 \partial^2 R}{\partial^2 x_{N+1}} + \frac{(v_1)(v_{N+1}) \partial^2 R}{\partial x_{N+1} \partial x_1}\right) + \cdots$$

$$\left(\frac{v_{N+N}^2 \partial^2 R}{\partial^2 x_{N+N}} + \frac{(v_N)(v_{N+N}) \partial^2 R}{\partial x_{N+N} \partial x_N}\right). \tag{A8}$$

Since there are similar expressions due to symmetry, it is sufficient to write this equation. When necessary adjustments are made in (A8), the following equation is finally obtained:

$$\mathbf{v}^{\mathrm{T}}\mathbf{H}\mathbf{v} = -\frac{y_3 y_4^2 \{(v_1 x_{N+1}) + (v_{N+1}(y_5 - x_1))\}^2}{\ln 2 (x_{N+1})(x_{N+1} + (y_5 - x_1) y_4)^2} - \frac{v_1^2 M y_2 z^2 x_1}{\ln 2 (x_1^2 + x_1 z)^2}. \quad (A9)$$

It can be easily seen that the above expression is $\mathbf{v}^{\mathrm{T}}\mathbf{H}\mathbf{v} \leq 0$. This result shows us that the $\mathbf{H}$ matrix is a negative semidefinitive matrix. Thus, we have proven that $R_{\mathrm{sum}}(\mathbf{x})$ is a concave function with respect to $\mathbf{x}$, it can be solved by convex optimization techniques and the optimal solution can be found.

Appendix B: Algorithm

The following algorithm can be applied separately for the proposed TDMA and NOMA scenarios as Equation (14) and Equation (17) are independent of each other.

Algorithm 1. Algorithm for TDMA and NOMA.

Step 1: In the harvest and relay selection mode, the number of transmitted data to relay users is compared to a predetermined threshold (R_{t}).

if $R_j^{\mathrm{s}} = \beta B_i^{\mathrm{b}} \gamma_i g_{ij} \geq R_{\mathrm{t}}$ **then**
    R_j^{s} is active
else
    R_j^{s} inactive
end if

Step 2: R_{sum_1} is obtained by determining the number of data transmitted to the SR in busy mode.

Step 3: R_{sum_2} is obtained by determining the number of data transmitted to the SR in idle mode.

Step 4: $R_{\mathrm{sum}} = R_{\mathrm{sum}_1} + R_{\mathrm{sum}_2}$ is maximized over $\boldsymbol{\phi}$ and $\boldsymbol{\tau}$.